Emergence of coherent structures in barotropic turbulence

Nikolaos A. Bakas[1] and Petros J. Ioannou[2]
[1] Department of Physics, University of Ioannina, [2] Department of Physics, National and Kapodistrian University of Athens
email: nbakas@uoi.gr

ABSTRACT

Planetary turbulence is observed to self-organize into large scale structures such as zonal jets and coherent vortices. One of the simplest models that retains the relevant dynamics of turbulent self-organization is a barotropic flow in a beta-plane channel with turbulence sustained by random stirring. Non-linear integrations of this model show that as the energy input rate of the forcing is increased, the homogeneity of the flow is first broken by the emergence of non-zonal, coherent, westward propagating structures and at larger energy input rates by the emergence of zonal jets. The emergence of both non-zonal coherent structures and zonal jets is studied using a statistical theory, Stochastic Structural Stability Theory (S3T). S3T models a second order approximation to the statistical mean state and allows identification of statistical equilibria and study of their stability. It is found that when the homogeneous turbulent state becomes S3T unstable, coherent structures emerge (non-zonal large scale structures and zonal jets). Analytic expressions for their characteristics (scale, amplitude and phase speed) are obtained and their non-linear equilibration is studied numerically. Direct Numerical Simulations of the nonlinear equations show that the structures predicted by S3T dominate the turulent flow.

Keywords: turbulence self-organization, statistical state dynamics, coherent structures

1. INTRODUCTION

Planetary turbulence is commonly observed to be organized into large scale zonal jets with long-lasting coherent vortices embedded in them. Prominent examples are the banded jets and the Great Red Spot in the Jovian atmosphere (Vasavada and Showman, 2005). The jets control the transports of heat and chemical species in the atmosphere, while the coherent vortices sequester chemical species and heat and produce significant spatiotemporal variability. It is therefore important to understand the mechanisms for the emergence, equilibration, and maintenance of these coherent structures.

The simplest model that retains the relevant dynamics is a turbulent barotropic flow on a β-plane. Numerical simulations of this model have shown that robust, large scale zonal jets emerge in the flow and are sustained at finite amplitude. In addition, large scale westward propagating coherent waves were found to coexist with the zonal jets (Galperin et al., 2010). These large scale waves either obey a Rossby wave dispersion, or propagate with different phase speeds and appear to be sustained by non-linear interactions between Rossby waves. However the mechanism for their excitation and maintenance remains elusive. In this work, we present a theory that predicts the formation and nonlinear equilibration of large scale coherent structures in barotropic β-plane turbulence and then test this theory against nonlinear simulations.

Since organization of turbulence into coherent structures involves complex nonlinear interactions among a large number of degrees of freedom, which erratically contribute to the maintenance of the large-scale structure, an attractive approach is to study the Statistical State Dynamics (SSD) of the turbulent flow, rather than single realizations of the turbulent field. This approach is followed in Stochastic Structural Stability Theory (S3T) which is a second order Gaussian approximation of the full SSD (Farrell and Ioannou, 2003). In S3T the third cumulant is either ignored (Marston et al., 2008) or parameterized as the sum of a known correlation function and a dissipation term (DelSole and Farrell, 1996), which is equivalent to the elimination of the eddy--eddy nonlinearity or its parameterization as random forcing with the required dissipation to remove the energy injected by the forcing. Such a representation is strongly supported by the results of previous studies (Farrell and Ioannou, 1993; DelSole, 2004; Bouchet et al., 2013).

The second order closure results in a nonlinear, autonomous dynamical system that governs the evolution of the mean flow and its consistent second order perturbation statistics. Its fixed points define statistical equilibria, whose instability brings about structural reconfiguration of the mean flow and of the turbulent statistics. Previous studies employing S3T addressed the bifurcation from a homogeneous turbulent regime to a jet forming regime in barotropic beta-plane turbulence and showed that S3T can predict the structure of zonal jets in the turbulent flow (Farrell and Ioannou, 2007, Srinivasan and Young, 2012, Constantinou et al., 2014). In this work we demonstrate that an extended version of S3T can predict the emergence of both zonal and non-zonal coherent structures and can capture their finite amplitude manifestations.

2. FORMULATION OF STOCHASTIC STRUCTURAL STABILITY THEORY

Consider a non-divergent barotropic flow on a β-plane with cartesian coordinates $\mathbf{x}=(x,y)$. The velocity field, $\mathbf{u}=(u,v)$, is given by $(u, v) = (-\partial_y\psi, \partial_x\psi)$, where ψ is the streamfunction. Relative vorticity $\zeta(x, y, t) = \Delta\psi$, evolves according to the non-linear (NL) equation:

$$(\partial_t + \mathbf{u}\cdot\nabla)\zeta + \beta v = -r\zeta - \nu\Delta^2\zeta + f \quad (1)$$

where $\Delta = \partial_{xx}^2 + \partial_{yy}^2$ is the horizontal Laplacian, β is the gradient of planetary vorticity, r is the coefficient of linear dissipation that typically parameterizes surface (Ekman) drag in planetary atmospheres and ν is the coefficient of hyper-diffusion that dissipates enstrophy flowing into unresolved scales. The exogenous forcing term f, parameterizes processes such as small scale convection or baroclinic instability, that are missing from the barotropic dynamics and is necessary to sustain turbulence in this simplified model that lacks vortex stretching. We assume that f is a temporally delta correlated and spatially homogeneous random stirring. We also assume that the forcing is isotropic, injecting energy at a rate ε in a narrow ring of wavenumbers with radius K_f.

We assume a standard Reynolds decomposition of the vorticity field into an averaged field $Z=T[\zeta]$, defined as a time average over an intermediate time scale and deviations from the mean or eddies, $\zeta'=\zeta-Z$. The intermediate time scale is larger than the time scale of the turbulent motions but smaller than the time scale of the large scale motions. With this decomposition, (1) is written as:

$$(\partial_t + \mathbf{U}\cdot\nabla)Z + \beta V + rZ + \nu\Delta^2 Z = -\nabla\cdot T[\mathbf{u}'\zeta'] \quad (2a)$$

$$(\partial_t + \mathbf{U}\cdot\nabla)\zeta' + v'\left(\beta + \partial_y Z\right) + u'\partial_x Z + r\zeta' + \nu\Delta^2\zeta' = f + \nabla\cdot\left(T[\mathbf{u}'\zeta'] - \mathbf{u}'\zeta'\right) \quad (2b)$$

As in previous studies (Srinivasan and Young 2012), we neglect the eddy-eddy term $(T[\mathbf{u}'\zeta'] - \mathbf{u}'\zeta')$ to obtain the quasi-linear system

$$(\partial_t + \mathbf{U}\cdot\nabla)Z + \beta V + rZ + \nu\Delta^2 Z = -\nabla\cdot T[\mathbf{u}'\zeta'] \quad (3a)$$

$$\partial_t \zeta' = A(\mathbf{U})\zeta' + f \quad (3b)$$

where $A = -\mathbf{U}\cdot\nabla - \left(\beta + \partial_y Z\right)\partial_x \Delta^{-1} + \partial_x Z \partial_y \Delta^{-1} - r + \nu\Delta^2$. Therefore the mean flow is forced by the time mean of the vorticity flux divergence, while the eddies evolve according to the linear dynamics about the instantaneous mean flow **U**. In order to obtain the statistical dynamics of the quasi-linear system (3) we make the ergodic assumption that the time average over the intermediate time scale is equal to the ensemble average over the forcing realizations, an assumption used previously in studies of atmospheric blocking (Bernstein and Farrell, 2009). Under this assumption, the slowly varying mean flow Z is also the first cumulant of the vorticity $Z = \langle\zeta\rangle$, where the brackets denote the ensemble average. In addition, the time mean of the vorticity flux is equal to the ensemble mean of the flux, $T[\mathbf{u}'\zeta'] = \langle\mathbf{u}'\zeta'\rangle$, which can be expressed as a linear function, *R(C)*, of the eddy vorticity covariance between points $\mathbf{x}_1$ and $\mathbf{x}_2$, $C(\mathbf{x}_1, \mathbf{x}_2) = \langle\zeta'(\mathbf{x}_1, t)\zeta'(\mathbf{x}_2, t)\rangle$**.** The first cumulant, *Z*, therefore evolves according to:

$$(\partial_t + \mathbf{U}\cdot\nabla)Z + \beta V + rZ + \nu\Delta^2 Z = -\nabla\cdot\langle\mathbf{u}'\zeta'\rangle = R(C) \quad (4a)$$

Taking the time derivative of *C* and using (3b) we obtain the evolution equation for the second cumulant *C*:

$$\partial_t C + (A_1 + A_2)C = \Xi \quad (4b)$$

where $\Xi(\mathbf{x}_1 - \mathbf{x}_2)$ is the spatial covariance of the homogeneous stochastic forcing and the subscript in *A* denotes that the coefficients of $A(\mathbf{U})$ are evaluated at $\mathbf{x}_i$ and that it acts only on the variable $\mathbf{x}_i$.

Equations (4) comprise the autonomous S3T system which constitutes a second-order closure for the flow statistics. Being autonomous it may possess statistical equilibria *(Z^E, C^E)* of the coherent structures with vorticity Z^E, in the presence of an eddy field with covariance C^E. If these equilibria are stable, we expect reflections of the coherent structures Z^E to appear in the nonlinear simulations of (1) and statistics of the eddies to be given by C^E. If these equilibria are unstable, we expect that the turbulent attractor will change its structure and that different structures will emerge and dominate the flow. The S3T system (4) has for *ν=0* the equilibrium $Z^E=0$, $C^E=\Xi/2r$, that has zero large scale flow and a homogeneous eddy field with the spatial covariance of the forcing. We will now investigate the stability of this equilibrium as a function of the energy input rate ε and the characteristics of the unstable structures.

3. STABILITY ANALYSIS

The stability of the homogeneous equilibrium is assessed by introducing perturbations $\delta Z = e^{inx + imy + \sigma t}$, $\delta C = e^{in(x_1+x_2)/2 + im(y_1+y_2)/2 + \sigma t}$, linearizing (4) about the homogeneous equilibrium and calculating the eigenvalues σ for each plane wave with wave-vector $\boldsymbol{n} = (n, m)$. The resulting stability equation for $\sigma(\boldsymbol{n})$ is:

$$\sigma + i\omega_{\boldsymbol{n}} + r = \iint_{-\infty}^{\infty} \frac{d^2\boldsymbol{k}}{(2\pi)^2} \frac{|\boldsymbol{k}\times\boldsymbol{n}|^2 (K_s^2 - K^2)(K^2 - N^2)\hat{\Xi}(\boldsymbol{k})}{K^4 K_s^2 N^2 [\sigma + 2r - i(\omega_{\boldsymbol{k}} - \omega_{\boldsymbol{k}+\boldsymbol{n}}\ ]} \quad (5)$$

where the integral is over wavenumbers $\boldsymbol{k} = (k, l)$, $K = |\boldsymbol{k}|$, $N = |\boldsymbol{n}|$, $K_S = |\boldsymbol{k} + \boldsymbol{n}|$, $\omega_{\boldsymbol{k}} = -\beta k/K^2$ is the Rossby wave frequency and $\hat{\Xi}(\boldsymbol{k}) = 4\pi\varepsilon K_f\, \delta\left(K - K_f\right)$ is the Fourier transform of the isotropic ring forcing with spatial covariance Ξ (Bakas and Ioannou 2014). For small values of the energy input rate of the forcing ε, the homogeneous state is stable. When ε exceeds a critical ε_c, the homogeneous flow becomes S3T unstable and coherent structures emerge. The critical energy input rate as a function of the planetary vorticity gradient β is shown in Fig. 1. For $\beta<\beta_{min}$, the most unstable structures are zonal jets that grow

in situ (i.e Im[$\sigma(\boldsymbol{n})$]=0). This is illustrated in Fig. 2 showing the growth rate and the frequency of the unstable structures as a function of the wavenumber. For $\beta>\beta_{min}$, non-zonal structures are more unstable than zonal jets (cf. Fig. 2). As a result, the non-zonal structures first emerge as ε increases (thick line in Fig. 1) and only at significantly higher energy input rates zonal jets are expected to appear (thin line in Fig. 1). The non-zonal structures are propagating (i.e Im(σ_i)≠0) (cf. Fig. 2) and for energy input rates close to the critical value, they propagate in the retrograde direction and follow the Rossby wave dispersion, that is Im[$\sigma(\boldsymbol{n})$]=$\omega_{\boldsymbol{n}}$.

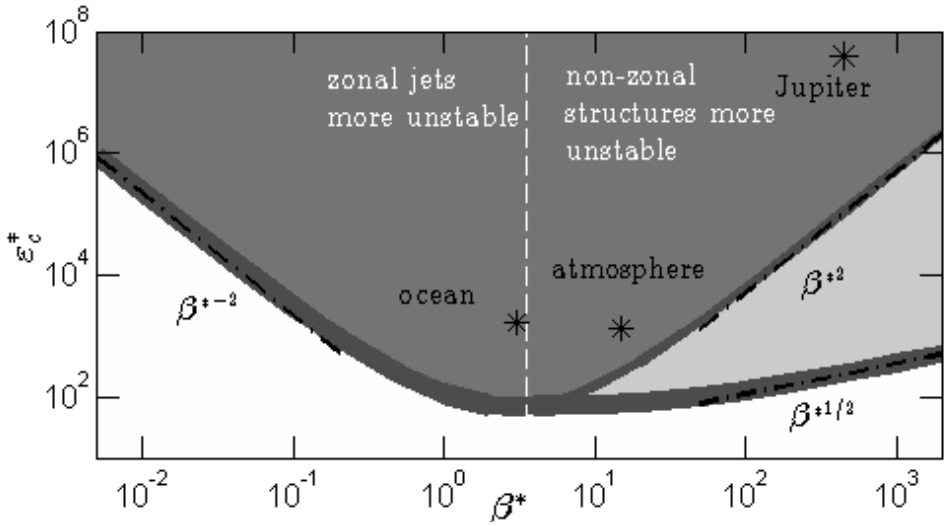

Fig. 1. The non-dimensional critical energy input rate $\varepsilon_c^* = \varepsilon_c K_f^2/r^3$ for the emergence of large-scale structure (thick line) and the critical energy input rate for the emergence of zonal jets (thin line) as a function of non-dimensional planetary vorticity gradient $\beta^* = \beta K_f/r$. The asymptotic behavior of the critical curve for $\beta^*>>1$ and $\beta^*<<1$ is also shown (dash-dot) and parameter values for the Earth's atmosphere, Earth's ocean and Jupiter's atmosphere are marked with stars.

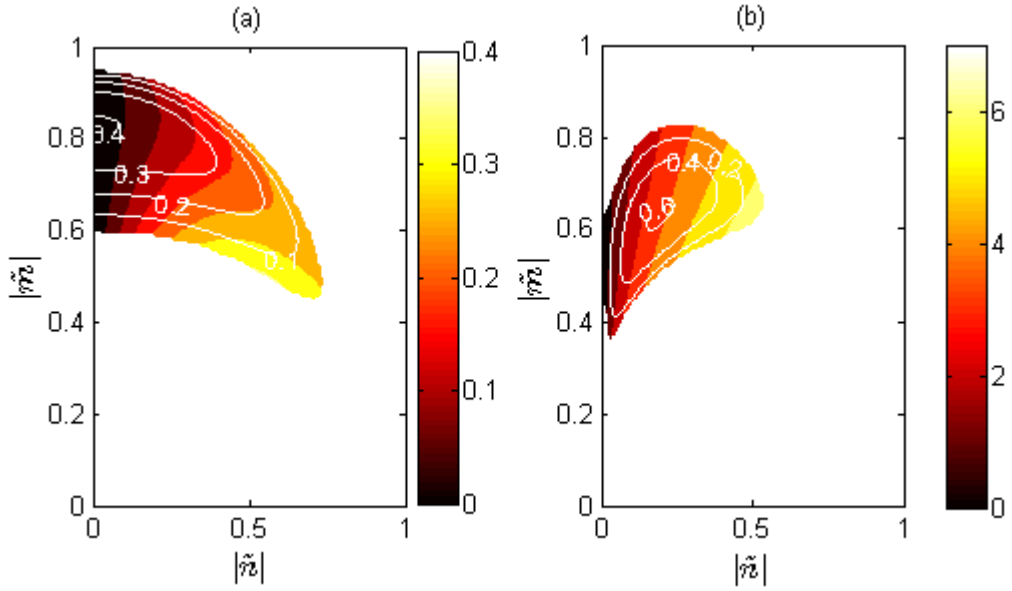

Fig. 2. Non-dimensional growth rate Re(σ/r) (contours) and frequency Im(σ/r) (shading) as a function of the integer valued non-dimensional wavenumbers ($|n|$,$|m|$)/K_f of the emerging structure for (a) β^*=1 and (b) β^*=1. The energy input rate in both panels is ε=2ε_c.

4. EQUILIBRATION OF THE INSTABILITIES AND COMPARISON TO DNS

The equilibration of the instabilities is studied by numerically integrating the S3T system (4) in a doubly periodic 2π x 2π channel using finite differences for calculating the spatial derivatives and a fourth-order Runge-Kutta scheme for time stepping. We consider the parameter values K_f=10, β=10, r=0.01 and ν=1.9x10^{-6} yielding a non-dimensional planetary vorticity gradient $\tilde{\beta} = 100$. Therefore the integration is in the parameter region of Fig. 1 in which the non-zonal structures are more unstable than zonal jets. The eigenvalue relation can be readily derived for a periodic channel by substituting the integrals with summation over integer values of the wavenumber $\boldsymbol{k} = (i, j)$, with $i, j \in \mathbb{Z}$.

We first consider the energy input rate ε=4ε_c for which zonal jets are stable and the structure with $\boldsymbol{n}$=(1, 5) is the most unstable. Starting from a small random perturbation, a checkerboard perturbation of the form

$$Z = \cos(x)\cos(5y) \qquad (6)$$

emerges and grows exponentially dominating the flow. At this point the large scale flow gets attracted to the travelling wave finite-amplitude equilibrium structure shown in Fig. 3 that is very close in form to the checkerboard unstable harmonic eigenfunction (6). The Hovmoller diagram of $\psi(x,y=\pi/4,t)$ also

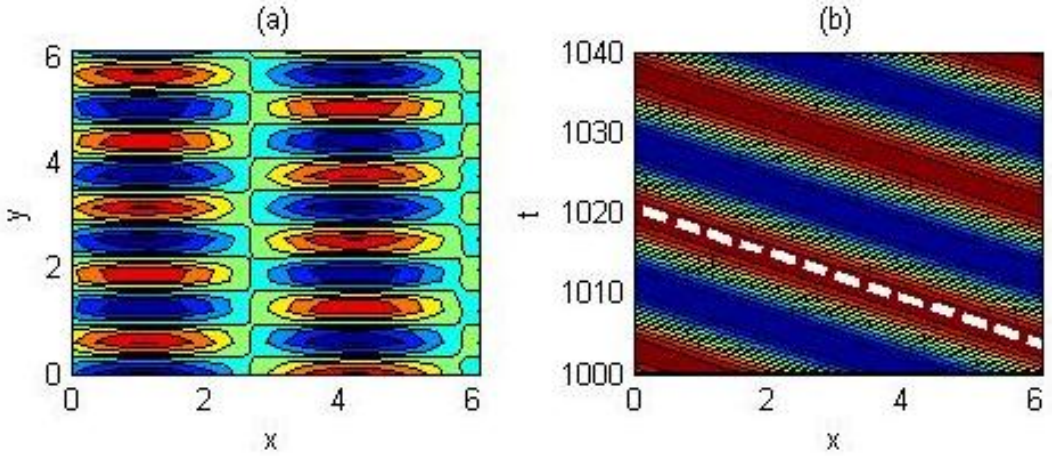

Fig. 3. (a) Streamfunction of the equilibrated structure for ε=4ε_c. (b) Hovmoller diagram of $\psi(x,y=\pi/4,t)$. The phase speed of the most unstable eigenfunction is also shown (dashed line).

shown in Fig. 3 illustrates that the wave propagates in the retrograde with a speed approximately equal to the phase speed of the unstable eigenfunction. We next consider the case ε=30ε_c. For this highly supercritical value of the energy input rate the most unstable non-zonal structure grows but cannot equilibrate as the finite-amplitude non-zonal travelling equilibria become S3T unstable to zonal jet perturbations. This is illustrated in Fig. 4 showing the evolution of the harmonic function (5). After the saturation of the instability at about t=100, the flow transitions slowly from the traveling wave structure (shown in the left inset in Fig. 4) to the equilibrium state shown in the right inset in Fig. 4. The equilibrated structure is a mixed state consisting of a zonal jet with ($|n|$, $|m|$)=(0,5) and lower amplitude ($|n|$, $|m|$)=(1,5) westward propagating waves embedded in it. Therefore we expect two regime changes as the energy input rate increases. The first occurring at ε_c with the emergence of non-zonal structures and the second with the dominance of the zonal jet-mixed states when the non-zonal structures become secondarily unstable. These two regime transitions can be clearly revealed by calculating two proxies for the amplitude of non-zonal structures and zonal jets, the zmf and nzmf

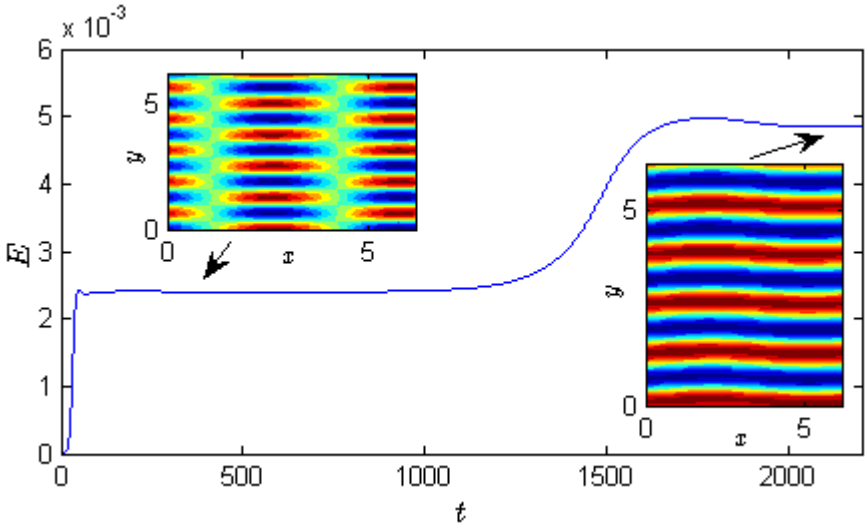

Fig. 4. Energy evolution of random initial conditions for $\varepsilon=30\varepsilon_c$. The insets show a snapshot of the streamfunction at t=200 (left) and t=2200 (right).

indices defined as the ratio of the energy of zonal jets and non-zonal structures respectively with scales lower than the scale of the forcing over the total energy:

$$zmf = \frac{\sum_{l<K_f} \hat{E}(k=0,l)}{\sum_{k,l} \hat{E}(k,l)}, \quad nzmf = \frac{\sum_{k,l<K_f} \hat{E}(k,l)}{\sum_{k,l} \hat{E}(k,l)} - zmf, \quad (7)$$

where $\hat{E}(k,l)$ is the time averaged energy power spectrum of the flow and k, l are the zonal (x) and meridional (y) wave numbers, respectively. These indices that are calculated for the S3T integrations, are shown in Fig. 5 as a function of the energy input rate ε. As the energy input rate increases, the non-

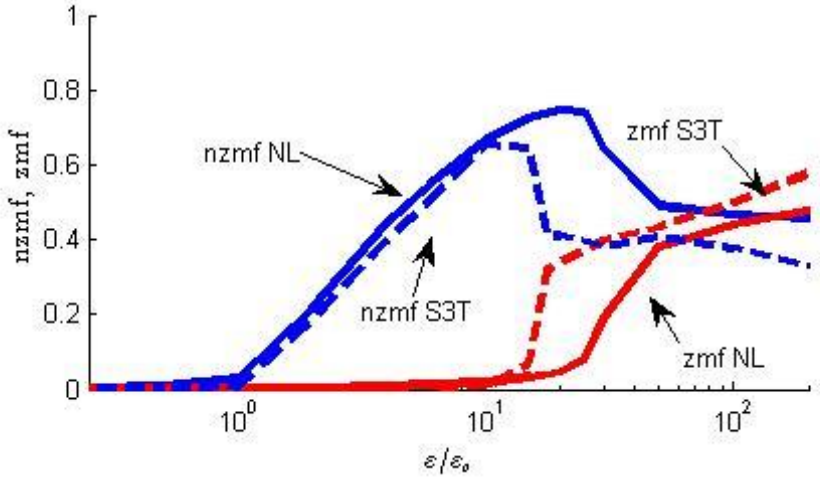

Fig. 5. zmf and nzmf indices defined in (7) as a function of the energy input rate, for the NL and S3T integrations.

zonal structures emerge for $\varepsilon>\varepsilon_c$ and equilibrate at larger amplitudes and nzmf increases. For $\varepsilon/\varepsilon_c>15$ the finite amplitude non-zonal equilibria are S3T unstable to zonal jet perturbations and the structures with the largest domain of attraction are the mixed states dominated by their zonal jet component resulting in an increase of zmf and a concomitant decrease of nzmf.

The results of the S3T analysis are now compared to Direct Numerical Simulations of (1). Equation (1) is solved using a pseudospectral code with a 128x128 resolution and a fourth-order Runge-Kutta scheme for time stepping and we choose the same parameters as in the S3T integrations. The zmf and nzmf indices calculated from long time averages after the system has reached a statistical equilibrium are shown in Fig. 5. We observe that the S3T stability analysis accurately predicts the critical ε_c for emergence of non-zonal structures in the DNS of the turbulent flow as well. The finite amplitude equilibria obtained when $\varepsilon>\varepsilon_c$ also correspond to the dominant structures in the nonlinear simulations. For $\varepsilon=4\varepsilon_c$, the time averaged energy spectra shown in Fig. 6 exhibit significant power at $(|k|,|l|)=(1,5)$, corresponding to the equilibrated S3T structure shown in Fig. 3. Remarkably, the phase speed of these waves observed in the nonlinear simulations and the amplitude of these structures as illustrated by the

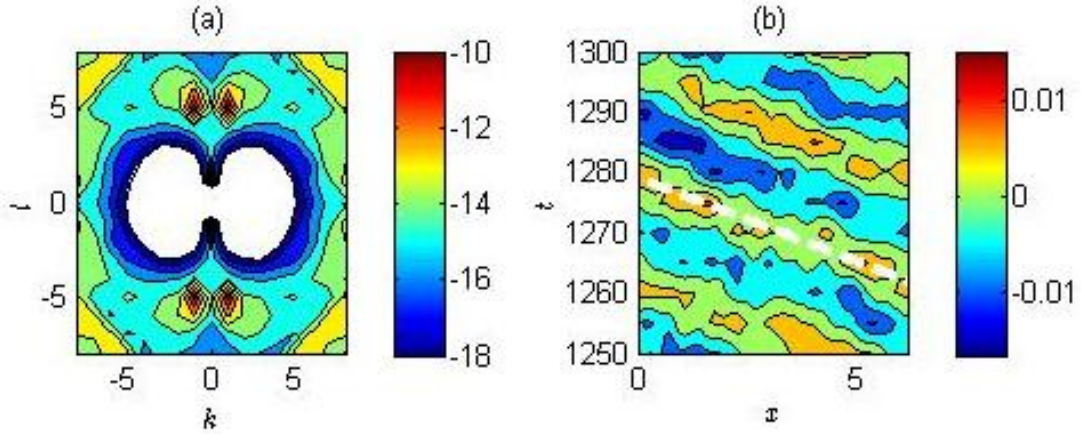

Fig. 6. (a) Time averaged energy power spectra obtained from the NL simulations for $\varepsilon=4\varepsilon_c$. (b) Hovmoller diagram of $\psi(x,y=\pi/4,t)$. The phase speed of the most unstable S3T eigenfunction in this case is also shown (dashed line).

nzmf index are approximately equal to the phase speed and amplitude of the corresponding S3T translating equilibrium structure (cf. Figs. 3, 6). An excellent agreement is also observed for the second regime as well in which zonal jets (mixed states) are the dominant structures. The energy spectra calculated at $\varepsilon=30\varepsilon_c$ (not shown) exhibit a peak at the zonal mode with $(|k|,|l|)=(0,5)$ but there is also finite power in the non-zonal structures with $(|k|,|l|)=(1,5)$, that is the two constituents of the mixed state in the S3T integrations. The amplitude of both the zonal and non-zonal components is also in good agreement with the S3T integrations as revealed by the comparison of the zmf and nzmf indices with the corresponding indices obtained from S3T in this regime (cf. Fig. 5).

5. CONCLUSIONS

In summary, we presented a theory for the emergence of zonal jets and non-zonal coherent structures in barotropic turbulence. Nonlinear simulations of a stochastically forced barotropic flow in a beta-plane channel show two major flow transitions as the energy input rate of the forcing increases. In the first, the translational symmetry in the flow is broken with the emergence of propagating coherent non-zonal waves that approximately follow the Rossby wave dispersion. The power in these non-zonal structures increases with the energy input rate until the second transition occurs with the emergence of robust zonal jets.

The two flow transitions and the characteristics of both the non-zonal structures and the zonal jets are investigated using S3T. In S3T, the turbulent flow dynamics and statistics are expressed as a systematic cumulant expansion which is truncated at second order. With the interpretation of the ensemble average as a Reynolds average over the fast turbulent eddies, the second-order cumulant expansion results in a closed, nonlinear dynamical system that governs the joint evolution of slowly

varying, spatially localized coherent structures with the second-order statistics of the rapidly evolving turbulent eddies.

The linear stability of the homogeneous S3T equilibrium with no mean velocity was examined analytically. Structural instability was found to occur when the energy input rate is larger than a certain threshold. It was found that for weak (strong) planetary vorticity gradient β the maximum growth rate occurs for stationary zonal structures (propagating large-scale non-zonal structures). The equilibration of the unstable, exponentially growing coherent structures for large β was then studied through numerical integrations of the S3T dynamical system. When the forcing amplitude is slightly supercritical, the finite-amplitude travelling wave equilibrium has a structure close to the corresponding unstable non-zonal perturbation with the same scale. When the forcing amplitude is highly supercritical, the instabilities equilibrate to mixed states consisting of strong zonal jets with smaller-amplitude travelling waves embedded in them.

The predictions of S3T were then compared with the results obtained in the nonlinear simulations. The critical threshold above which coherent non-zonal structures are unstable according to the stability analysis of the S3T system was found to be in excellent agreement with the critical value above which non-zonal structures acquire significant power in the nonlinear simulations. The scale, phase speed and amplitude of the dominant structures in the nonlinear simulations were also found to correspond to the structures predicted by S3T. In addition, the threshold for the emergence of jets, which is identified in S3T as the energy input rate at which an S3T stable, finite-amplitude zonal jet equilibrium exists, was found to roughly match the corresponding threshold for jet formation in the nonlinear simulations, with the emerging jet scale and amplitude being accurately obtained using S3T.

In summary, S3T predicts the two regime transitions in the turbulent flow as the energy input rate is increased: the emergence of coherent, propagating non-zonal structures and the emergence of zonal jets. It also predicts the characteristics of the emerging structures (their scales and their phase speed), as well as their amplitude.

References

Bakas, N. A., and P. J. Ioannou (2014) A theory for the emergence of large scale structures in beta-plane turbulence. J. Fluid Mech. 740, 312

Bernstein, J. and B. F. Farrell (2009) Low frequency variability in a turbulent baroclinic jet: eddy-mean flow interactions in a two-level model. J. Atmos. Sci. 67:452–467

Bouchet, F., Nardini, C. and T. Tangarife (2013) Kinetic theory of jet dynamics in the stochastic barotropic and 2D Navier–Stokes equations. J. Stat. Phys. 153, 572–625.

Constantinou NC,Farrell BF and Ioannou PJ (2014) Emergence and equilibration of jets in barotropic beta-plane turbulence: applications of Stochastic Structural Stability Theory. J. Atmos. Sci., 71(5), 1818-1842.

DelSole, T. (2004) Stochastic models of quasigeostrophic turbulence. Surv. Geophys. 25, 107–194.

DelSole, T. and B. F. Farrell (1996) The quasi-linear equilibration of a thermally maintained, stochastically excited jet in a quasigeostrophic model. J. Atmos. Sci. 53, 1781–1797.

Farrell, B. F. and P. J. Ioannou (1993) Stochastic dynamics of baroclinic waves. J. Atmos. Sci. 50, 4044–4057.

Farrell, B. F., and P. J. Ioannou (2003) Structural stability of turbulent jets. J. Atmos. Sci. 60:2101-2118

Farrell, B. F. and P. J. Ioannou (2007) Structure and spacing of jets in barotropic turbulence. J. Atmos. Sci. 65:3352-3355

Marston, J. B., Conover, E. and T. Schneider (2008) Statistics of an unstable barotropic jet from a cumulant expansion. J. Atmos. Sci. 65, 1955–1966.

Galperin BH, Sukoriansky S and Dikovskaya N (2010) Geophysical flows with anisotropic turbulence and dispersive waves: flows with a β-effect. Ocean Dyn. 60:427–441

Srinivasan, K. and W. R. Young (2012) Zonostrophic instability. J. Atmos. Sci. 69, 1633–1656.
Vasavada, A. R. and A. P. Showman (2005) Jovian atmospheric dynamics. An update after Galileo and Cassini. Rep. Prog. Phys. 68, 1935–1996.